Hindawi
International Journal of Photoenergy
Volume 2017, Article ID 4501758, 8 pages
https://doi.org/10.1155/2017/4501758

Research Article

Enhanced Efficiency of PTB7 : $PC_{61}BM$ Organic Solar Cells by Adding a Low Efficient Polymer Donor

Joana Farinhas,[1] Ricardo Oliveira,[1] Quirina Ferreira,[1] Jorge Morgado,[1,2] and Ana Charas[1]

[1]*Instituto de Telecomunicações, Instituto Superior Técnico, Av. Rovisco Pais, 1049-001 Lisboa, Portugal*
[2]*Department of Bioengineering, Instituto Superior Técnico, Universidade de Lisboa, Av. Rovisco Pais, 1049-001 Lisboa, Portugal*

Correspondence should be addressed to Jorge Morgado; jorge.morgado@lx.it.pt and Ana Charas; ana.charas@lx.it.pt

Received 16 September 2016; Accepted 18 December 2016; Published 11 January 2017

Academic Editor: Yulia Galagan

Ternary blend polymer solar cells combining two electron-donor polymers, poly[4,8-bis[(2-ethylhexyl)oxy]benzo[1,2-b:4,5-b′]dithiophene-2,6-diyl][3-fluoro-2-[(2-ethylhexyl)carbonyl]thieno[3,4-b]thiophenediyl] (PTB7) and poly[2,5-bis(3-dodecylthiophen-2-yl)thieno[3,2-b]thiophene] (pBTTT) and [6,6]-phenyl-C61-butyric acid methyl ester ($PC_{61}BM$), as electron-acceptor, were fabricated. The power conversion efficiency of the ternary cells was enhanced by 18%, with respect to the reference binary cells, for a blend composition with 25% (wt%) of pBTTT in the polymers content. The optimized device performance was related to the blend morphology, nonrevealing pBTTT aggregates, and improved charge extraction within the device.

1. Introduction

Polymer photovoltaic cells have demonstrated great potential as a cost-effective energy solar technology with unique characteristics of light weight and mechanical flexibility. In the last decade, the power conversion efficiency (PCE) of such cells improved remarkably; however, the highest values are still around 10–12% [1–5]. One of the main causes of the relatively low efficiency of polymer solar cells is incomplete harvesting of solar photons, which is due to the relatively narrow absorption spectrum of the polymer donor and the low absorption of the fullerene acceptor in the visible spectral range. To overcome such limitations, the so-called multi-donor solar cells, incorporating multiple organic polymers with different energy gaps and tandem cells [3], have been explored. However, to this respect, multidonor solar cells are the preferred option since they are single cell devices and therefore require a simpler fabrication process than tandem cells.

Typically, ternary bulk heterojunction (BHJ) cells combine a predominant donor : acceptor (D : A) system and a third component whose properties enable to pursuit higher efficiency. Thus, several types of third materials for several tasks have been effectively tested, as high-band gap polymers to enlarge the photon absorption window of the cell [6], dyes to harvest photons at longer wavelengths [7], additives to favour the optimal morphology of the BHJ [8], and cross-linkers to stabilize the device performance [9, 10].

In this work, ternary blends combining the low-band gap polymer donor PTB7 (E_g of *ca.* 1.6 eV), the fullerene acceptor $PC_{61}BM$, and a second polymer donor, pBTTT, were investigated and tested in BHJ solar cells. pBTTT is a semicrystalline polymer exhibiting remarkably high hole mobility (μ_{FET} up to 1 cm^2/Vs [11–13]) and absorption spectrum complementary to that of PTB7. For comparison, the reported values for the hole mobility of PTB7 in neat film are several orders of magnitude lower, in the range of 10^{-4}–10^{-3} cm^2/Vs, varying with the method of measurement [14–16]. These two properties potentially lead to a superior charge transport and enlarged photon harvesting, respectively, when pBTTT is added to the PTB7 : fullerene active layer. Previously reported studies of photovoltaic (PV) cells based on pBTTT and fullerenes showed poor performances, with maximum PCE values of 1-2% [17–19], probably caused by the high energy gap of pBTTT (E_g of *ca.* 1.9 eV). On the contrary, PTB7 is a high performing polymer in solar cells, yielding efficiencies as high as 9.2% with the acceptor $PC_{71}BM$ [20] and *ca.* 4–6% with $PC_{61}BM$ [21–23]. A few ternary solar cells based on PTB7 with a

second donor polymer and $PC_{71}BM$ showed efficiencies that surpassed the reference binary devices [24–29]. Nevertheless, only one work is reported on ternary systems based on PTB7 and $PC_{61}BM$, this being with poly(3-hexyl)thiophene (P3HT) as the second polymer and exhibiting only 4% in efficiency [30].

Here, five ternary blend compositions were tested, maintaining the polymers : $PC_{61}BM$ weight ratio as 1 : 2, and varying the relative polymer content, PTB7 : pBTTT, from 1 : 9 to 9 : 1 by weight. Reference binary blend cells, PTB7 : $PC_{61}BM$ and pBTTT : $PC_{61}BM$, were also fabricated and tested. The effect of pBTTT addition on the morphology of the cells' active layer was investigated by Atomic Force Microscopy (AFM) and fluorescence studies were made to assess the role of pBTTT.

2. Experimental

2.1. Materials and Device Fabrication. pBTTT and PTB7 were purchased from Ossila Ltd. $PC_{61}BM$ (99.55%) was purchased from Solenne BV. The devices were prepared on ITO-coated (100 nm thick) glass substrates (ITO: indium-tin-oxide) previously cleaned sequentially with distilled water and a nonionic detergent, distilled water, acetone, and isopropyl alcohol under ultrasounds. The ITO surface was submitted to UV-oxygen plasma for 3 minutes prior to spin casting poly(3,4-ethylenedioxythiophene) : polystyrene sulfonic acid (PEDOT : PSS) from aqueous dispersion (Clevios P VP.AI 4083, from Heraeus). The glass/ITO/PEDOT : PSS substrates were then dried over a hot plate at 125°C for 10 min. The blend solutions for the active layers of the cells were prepared by mixing adequate volumes of separate solutions containing the polymers and $PC_{61}BM$ in 1,2-dichlorobenzene (DCB), in order to achieve polymers : $PC_{61}BM$ mass ratio of 1 : 2. Five blend compositions, with total concentration of 40 mg·mL^{-1}, containing both polymers and $PC_{61}BM$, were prepared, where PTB7 : pBTTT weight ratio was varied from 9 : 1 to 1 : 9. The starting solutions of the pristine materials had the same concentration and were stirred for 3 h at 75°C. The blend solutions were further stirred for 3 h at 75°C before their deposition by spin coating (1800 rpm, 45 s) on either PEDOT : PSS-coated quartz substrates (for UV-Vis absorption measurements) or ITO/PEDOT : PSS substrates. For comparison purposes, the binary blends solutions were deposited under the same conditions. The thicknesses of the active layers varied from *ca.* 80 nm (for binary blend films of PTB7 : $PC_{61}BM$ and ternary blend films with 50%, 75%, and 90% of PTB7) to *ca.* 130 nm (for binary blend films of pBTTT : $PC_{61}BM$ and ternary blend films with 80% and 90% of pBTTT). Following the deposition of the active blends, LiF (1.5 nm) and Al (100 nm) were thermally evaporated on top, under a base pressure of 2×10^{-6} mbar, defining a device area of 0.24 cm^2.

2.2. Measurements. AFM studies were performed on a Nano Observer from Concept Scientific Instruments (Les Ulis, France), operating in noncontact mode, with cantilevers having a resonance frequency between 200 and 400 kHz and silicon probes with tip radius smaller than 10 nm. All images were obtained with 256 × 256 pixels resolution and processed using Gwyddion (version 2.26) software. UV-Vis absorption spectra were recorded on a Cecil 7200 spectrophotometer. Film thicknesses were measured with a Dektak 6M profilometer. Fluorescence spectra were acquired using a SPEX Fluorolog 212I, collecting the emission at a right angle arrangement in the R/S mode. All fluorescence spectra were corrected for the wavelength response of the instrumental system. The current-voltage (I-V) curves of the cells were measured under inert atmosphere (N_2) using a K2400 source-measure unit. The curves under illumination were measured with a solar simulator with 100 mW/cm^2 AM1.5G illumination (Oriel Sol 3A, 69920, Newport). At least 16 devices of each condition were prepared. The light intensity of the solar simulator was verified using a calibrated solar cell. External quantum efficiency (EQE) spectra were obtained under short-circuit conditions, using a homemade system with a halogen lamp as light source.

3. Results and Discussion

3.1. Photophysical Properties. Figure 1 shows the UV-Visible absorption and photoluminescence spectra of spin cast films of PTB7, pBTTT, and $PC_{61}BM$ on quartz substrates and the relative position of their HOMO and LUMO levels [17, 20, 31] with respect to the work functions of the electrodes of the fabricated cells.

The absorption spectrum of pBTTT shows a band which is blue-shifted (maximum at 535 nm) with respect to the main absorption band of PTB7 (maximum at 675 nm), thus potentially providing complementary photon absorption for the ternary cells comprising the two polymers. Since the emission of pBTTT overlaps the absorption band of PTB7, pBTTT may also sensitize PTB7, via excited state energy transfer. The energy diagram for the ternary cells shows a «cascade» of energy levels, where several pathways for the charge transfer are energetically favourable: the photoexcited pBTTT may transfer electrons to both fullerene ($PC_{61}BM$) and PTB7, and the photoexcited PTB7 can transfer electrons to $PC_{61}BM$. Thus, in other words, both polymers can act as electron-donors with respect to $PC_{61}BM$, contributing to the charge generation at the pBTTT/$PC_{61}BM$ and PTB7/$PC_{61}BM$ interfaces. However, it is not clear if the small mismatch of 0.2 eV between the LUMO energies of the two polymers is sufficient to promote the dissociation of the excitons generated within pBTTT at its interface with PTB7.

We have carried out photoluminescence studies on films of the ternary blends and also on films of blends composed of the two polymers only. The films were always in the same position in the spectrofluorometer cavity to minimize orientation effects. Films of the PTB7 : pBTTT blends without $PC_{61}BM$ were excited at the pBTTT absorption maximum (*ca.* 540 nm). The obtained fluorescence spectra showed no evidence of pBTTT emission, being only observed PTB7 fluorescence (see Figure S1 in Supplementary Material available online at https://doi.org/10.1155/2017/4501758). Figure 2 shows the PL spectrum when only 10% of PTB7 is present. The absence of pBTTT emission indicates that excited state

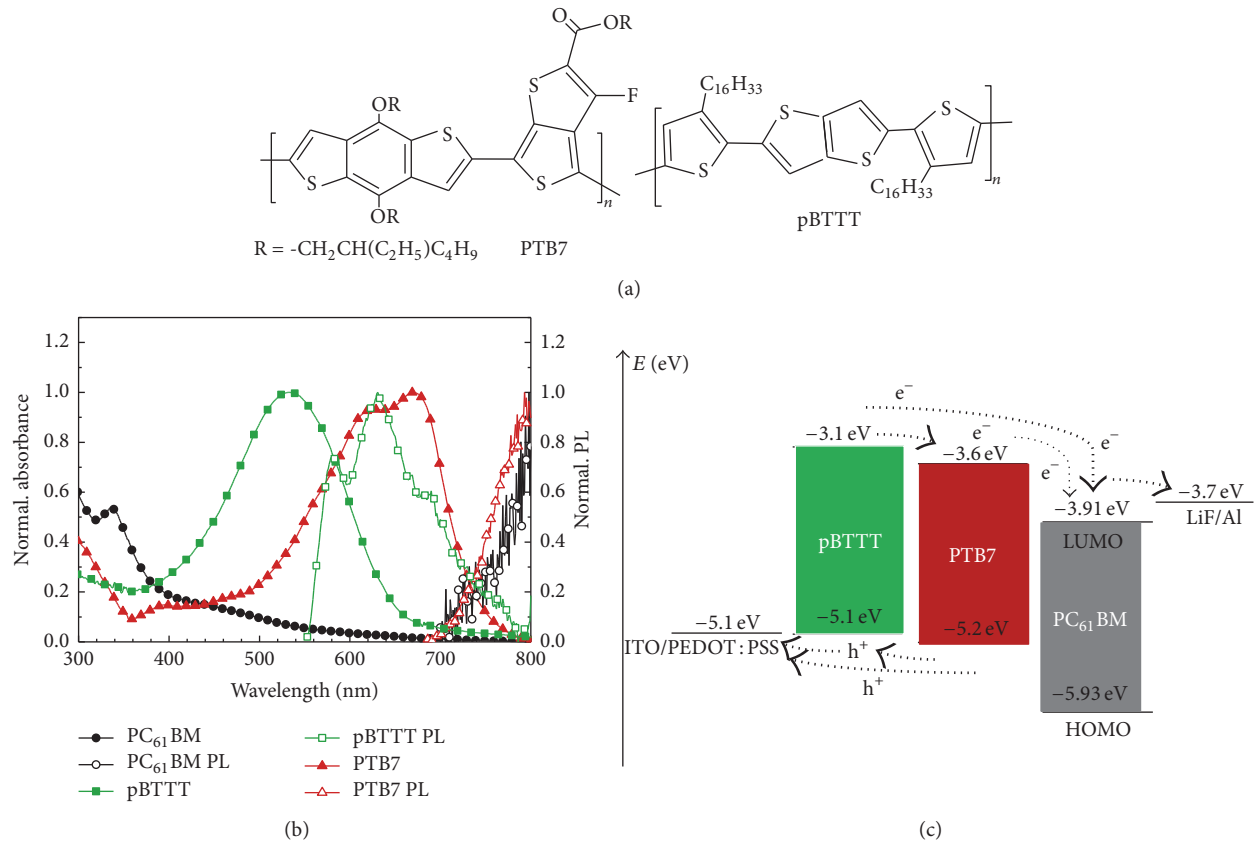

FIGURE 1: (a) Chemical structures of the two polymers, PTB7 and pBTTT. (b) Normalized UV-Visible absorption spectra (filled symbols) of films of $PC_{61}BM$, pBTTT, and PTB7 and corresponding PL spectra (open symbols) recorded upon excitation at 330 nm ($PC_{61}BM$), 535 nm (pBTTT), and 675 nm (PTB7) and (c) energy diagram of the ternary blend cells.

energy transfer and/or charge transfer from pBTTT to PTB7, as previewed by the optical properties and the frontier energy levels of the polymers, should effectively contribute to the decay of excitons photogenerated in pBTTT, although the relative importance of the two mechanisms cannot be inferred from these studies. It should be mentioned that PTB7 is also absorbed at 540 nm; thus the recorded emission results from the PTB7 direct excitation and possible energy transfer from pBTTT. We also observe that when $PC_{61}BM$ is added (reproducing the composition of the solar cells active layer) the PTB7 emission is quenched, which should be likely attributed to exciton dissociation at PTB7/$PC_{61}BM$ interface.

3.2. Photovoltaic Cells. The photovoltaic cells had the ITO/PEDOT : PSS/active layer/LiF/Al general structure, where the active layer is made of either the reference binary blends, PTB7 : $PC_{61}BM$ and pBTTT : $PC_{61}BM$, or the ternary layers based on PTB7 : pBTTT : $PC_{61}BM$. The cells performance parameters and the representative *J-V* curves obtained under illumination conditions (P_{in} = 100 mW·cm^{-2}) are shown in Table 1 and Figure 3, respectively (*J-V* curves measured under dark conditions are shown in Supplementary Material, Figure S2).

Regarding the pBTTT : $PC_{61}BM$ binary blend devices, the found PCE of 0.57% and V_{OC} of 0.5 V little surpass the reported values (*ca.* 0.5% and 0.45 V, resp.), while J_{SC} and FF are similar [17]. It should be noted that, according to reported works [18, 19], the blend composition 1 : 2 is not the most efficient one for this system, being the highest performances achieved for the 1 : 4 ratio using either $PC_{61}BM$ or $PC_{71}BM$. This enhancement in cells performance with higher PCBM content should be related to the presence of relatively pure PCBM phases which provide continuous conductive pathways for the electrons [19]. In this work, the 1 : 4 blend composition was also tested, resulting in devices with PCE of 1.07%, V_{OC} of 0.51 V, J_{SC} of 4.74 mA·cm^{-2}, and FF of 0.44%. Nevertheless the control devices were based on 1 : 2 blends in order to keep the mass ratio of D : A constant in both binary and ternary devices. Taking PTB7 : $PC_{61}BM$ as the reference system, we find that the partial replacement of PTB7 by pBTTT leads to a decrease in PCE with the exception of the composition 0.75 : 0.25 (PTB7 : pBTTT), which leads to the best performing cell. The reached PCE value (4.73%) corresponds to an improvement of *ca.* 18% over the binary cells. The maximum PCE obtained, 4.72%, surpasses the reported values for ternary systems based on PTB7 and $PC_{61}BM$ [30]. We also observe that, on the other

Table 1: Performance parameters of representative curves and maxima PCE values of the OPV cells.

PTB7 : pBTTT : $PC_{61}BM$	J_{SC} (mA·cm^{-2})	V_{OC} (V)	FF	PCE (%) rep./max	R_{sh} (Ω·cm^2)	R_s (Ω·cm^2)
0 : 1 : 2	2.59	0.50	0.44	0.57/0.66	457	40
0.10 : 0.90 : 2	4.15	0.55	0.39	0.90/1.08	311	50
0.20 : 0.80 : 2	5.27	0.54	0.39	1.11/1.24	1228	31
0.50 : 0.50 : 2	10.56	0.62	0.51	3.42/3.89	493	18
0.75 : 0.25 : 2	13.25	0.69	0.50	4.73/5.50	592	15
0.90 : 0.10 : 2	11.03	0.71	0.49	3.87/4.21	309	16
1 : 0 : 2	13.17	0.77	0.40	4.00/4.42	222	127

hand, all ternary cells show higher PCE than the cell based on pBTTT : $PC_{61}BM$.

Comparing the parameters characterizing the best performing ternary cell with those of the binary cell of PTB7 : $PC_{61}BM$, we find a slight increase of the short-circuit current. However it is the fill factor that improves significantly (from 0.40 to 0.50). This enlarged FF indicates that charge transport and/or charge collection were improved in the cells. In fact, the calculated values for R_{sh} and R_s for such cell are the most favourable within the series; that is, R_{sh} is maximum and R_s is minimum, thus indicating that recombination pathways for the charges are minimized and charge transport towards the electrodes is facilitated, respectively. The similar values of J_{SC} for the two most efficient cells, the ternary cell with 0.75 : 0.25 : 2 composition, and the binary cell of PTB7 : $PC_{61}BM$, being 13.17 mA·cm^{-2} and 13.25 mA·cm^{-2}, respectively, suggest that photon-to-charge conversion efficiency was only a little improved. Devices with a content of pBTTT higher than 25% showed the lowest currents and the poorest performances, probably due to energy losses caused by the high energy band gap of pBTTT and its consequent little contribution to photon absorption. Along the series, V_{OC} varies monotonically with the blend composition (except for the 0.2 : 0.8 : 2 case, with a V_{OC} of 0.54 that is slightly lower than the 0.55 V for the 0.10 : 0.90 : 2). The variation of V_{OC} with the blend composition in ternary blend cells has been rationalised in terms of an alloy model in which the donor/acceptor interface and corresponding interface band gap (charge transfer state) display a material averaged electronic structure, due to the delocalized nature of the one electron states [32].

The external quantum efficiency (EQE) spectra of the cells and the UV-Visible absorption spectra obtained for the respective active layers are shown in Figure 4.

We observe that the cells with the pBTTT binary blend and with the ternary blends with 90 and 80 wt% of pBTTT exhibit EQE spectra with a maximum at *ca.* 550 nm and with vibronic structure that mimics the UV-Visible absorption spectra of the respective blends. Such vibronic structure is not evidenced in the neat pBTTT film absorption spectrum (as shown in Figure 2), being likely attributed to ordering effects induced by the intermixing with the fullerene. In particular, several studies have demonstrated that pBTTT and $PC_{61}BM$ in blend films form cocrystals of approximately equal content

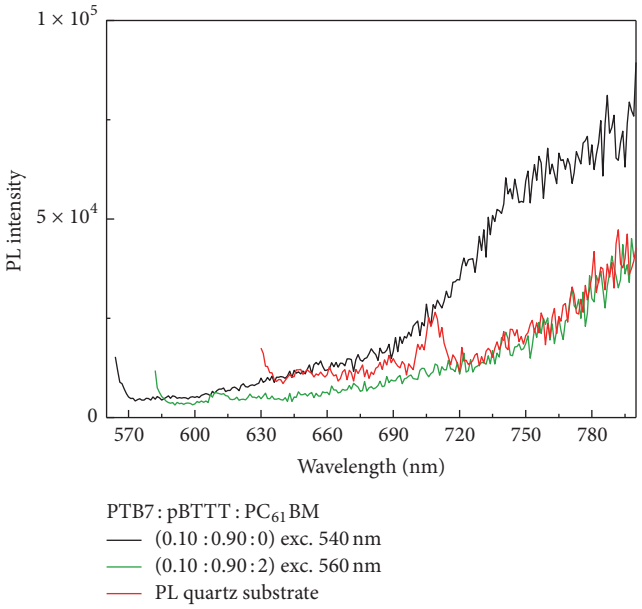

Figure 2: Photoluminescence spectra of films of the PTB7 : pBTTT (0.1 : 0.9) blend and of the same blend upon addition of $PC_{61}BM$, deposited over quartz substrates, following excitation at the maximum of absorption of pBTTT. For comparison, the spectrum of the bare quartz is also shown.

of polymer and fullerene which result in vibronic resolution in the absorption spectra [33, 34]. The presence of such cocrystals in the 1 : 2 binary blend may justify the lower efficiency of the corresponding cells in comparison with the tested 1 : 4 pBTTT : $PC_{61}BM$ cells, since less percolation pathways for electrons should be formed. The ternary devices with the highest efficiency (0.75 : 0.25 : 2) do not seem to gain significantly from the presence of pBTTT, since its EQE spectrum is very close to that of the binary cells with PTB7 : $PC_{61}BM$. This result is in agreement with the similar values of J_{SC} obtained for such cells. In fact, it is the fill factor that mainly causes the PCE enhancement with respect to the binary PTB7 : $PC_{61}BM$ cell when pBTTT is 25% of the total of polymers.

In view of the energy band diagram shown in Figure 1, cells with active layers composed of the two polymers only

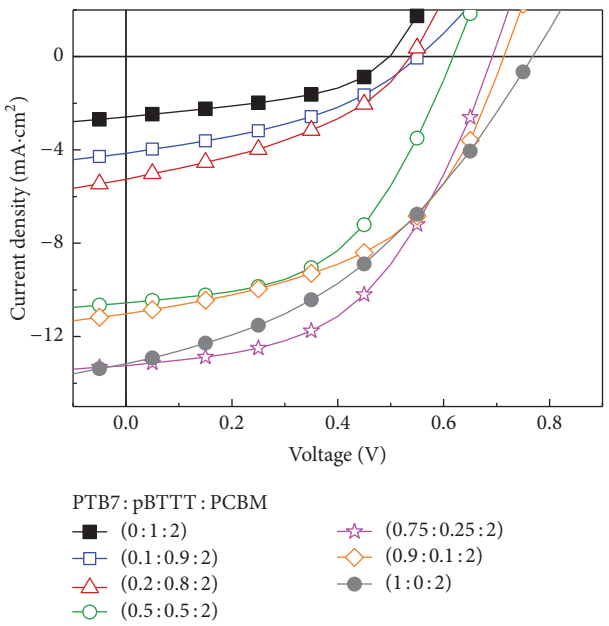

Figure 3: Current density-voltage (J-V) curves under AM 1.5G illumination (100 mW·cm^{-2}) of PV cells with active layers of PTB7 : $PC_{61}BM$ (1 : 2), pBTTT : $PC_{61}BM$ (1 : 2), and five ternary blend active layers with different PTB7 : pBTTT weight ratios.

(without $PC_{61}BM$) were also fabricated in order to evaluate the role of $PC_{61}BM$ in the cells and the importance of charge transfer at pBTTT/PTB7 interfaces. Hence, three types of devices with the ITO/PEDOT : PSS/active layer/LiF/Al structure were fabricated with 0.1 : 0.9, 0.5 : 0.5, or 0.9 : 0.1 (w/w) of PTB7 : pBTTT blends. The J-V curves of the devices, measured under the same conditions of illumination than those used for the ternary blend cells, exhibited J_{SC} values rather low, at the order of 10^{-2} mA/cm^2 (shown in Figure S3 in Supplementary Material). This confirms that $PC_{61}BM$ should be the main acceptor in the fabricated ternary blend cells and also suggests that if exciton dissociation between pBTTT and PTB7 interfaces exists, it should be an inefficient process.

3.3. Morphologic Characterization of Active Blends. Figure 5 shows the AFM topography and phase images of the reference binary blends and of the most efficient cell, with the ternary 0.75 : 0.25 : 2 (PTBT : pBTTT : $PC_{61}BM$) blend. The AFM images for the other ternary cells are shown in Supplementary Material (Figure S4). The variation of the surface roughness, R_{rms}, for all the seven films, as a function of the blend composition is represented in Figure 5(d).

The binary PTB7 : $PC_{61}BM$ blend shows a smooth and relatively homogeneous surface without evidencing phase segregated domains at the surface. However, the topography image of the binary pBTTT : $PC_{61}BM$ blend reveals a more structured surface and a much higher R_{rms} (*ca.* 1.37 nm), thus suggesting the presence of segregated domains of one of the materials. Since the corresponding phase image is relatively well homogeneous, such domains should exist within the bulk of the blend film. The AFM images of the ternary blend films with the highest contents of pBTTT (90% and 80%) show also similar domains (see Figure S3). The average dimensions of such segregated domains can be estimated from profile lines acquired from the AFM topographic images (Figure S5 in Supplementary Material). These are at the order of ca. 20 nm, thus indicating a lower degree of mixing between the polymer pBTTT and PCBM in comparison with the PTB7 : $PC_{61}BM$ binary blend films, where, as mentioned, the smooth films' surface does not evidence aggregates.

The R_{rms} calculated for the various films as a function of the pBTTT content shows that the R_{rms} values increase with the pBTTT content, although a slightly lower value is found when pBTTT is the sole polymer within the blend. We therefore suggest that aggregates of pBTTT have a negative effect on the pBTTT contribution to charge extraction, this leading to the lower fill factors found for the cells with higher pBTTT content. On the other hand, the addition of pBTTT in low contents (up to 50%), leading to rather smooth surfaces, should be related to an increase of the fill factors due to a positive contribution of pBTTT to hole extraction (since pBTTT is a good hole transport polymer) within the active blends. When pBTTT becomes the dominant polymer, FF decreases, a behavior that is accompanied by an increase of the surface roughness. These lower FF values, obtained when pBTTT is 90 or 80%, may be related to the presence of PTB7 in low contents that disrupts the favourable (to charge transport) pBTTT : PCBM phase, containing cocrystals and PCBM extended phases. The above-mentioned observation of vibronic structure on the pBTTT absorption and EQE is also consistent with such ordering in the blends when pBTTT is the dominant polymer.

4. Conclusions

Ternary BHJ solar cells based on PTB7 : pBTTT : $PC_{61}BM$ with improved PCE were demonstrated. The cells characteristics showed an enhancement in PCE for the ternary blends with 25% of pBTTT (wt% in polymers) of *ca.* 18% comparing with reference binary cells, yielding a PCE of 4.72%. The observed improvement was related to the optimal balance between the two polymers, providing higher FF values, and the absence of aggregates of pBTTT within the ternary blends. Also, according to PL steady state studies, energy and/or charge transfer processes from excited pBTTT to PTB7 should occur in the active layers of the ternary blend cells.

Competing Interests

The authors declare that they have no competing interests.

Acknowledgments

This work was supported by Fundação para a Ciência e Tecnologia (FCT), under Projects M-ERA.NET/0001/2012 and UID/EEA/50008/2013.

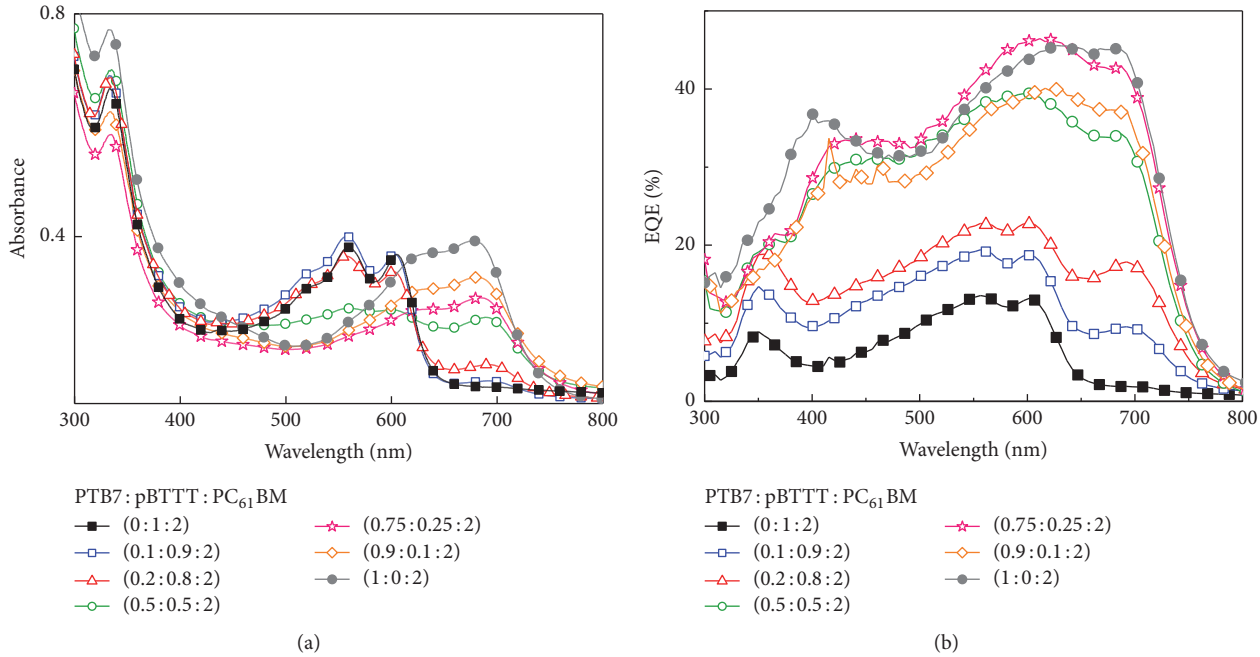

FIGURE 4: (a) UV-Visible absorption spectra of D : A binary blends and ternary blends deposited onto quartz/PEDOT : PSS substrates. (b) EQE spectra of the corresponding solar cells.

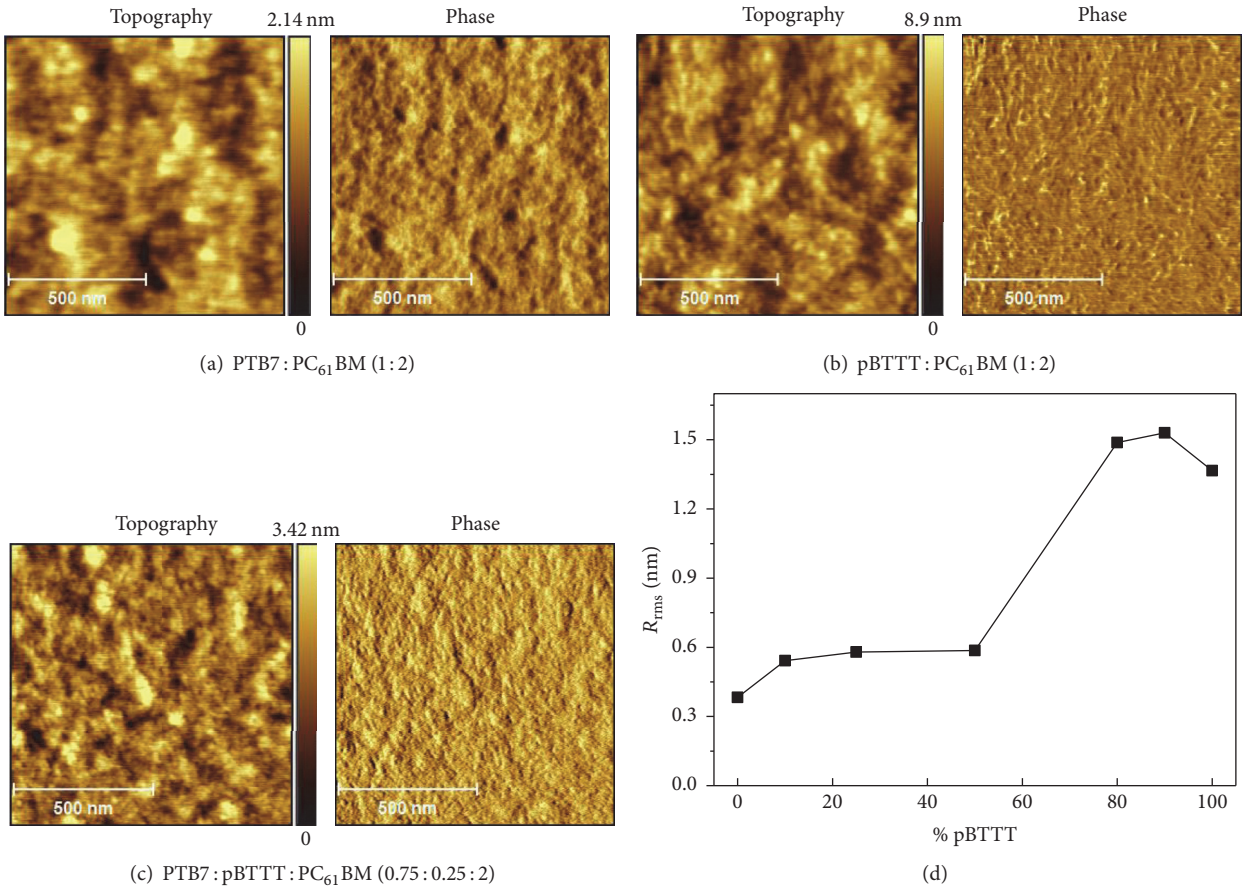

FIGURE 5: AFM topographic and phase images ($1 \times 1\,\mu m^2$) of (a) PTB7 : PC_{61}BM (1 : 2); (b) pBTTT : PC_{61}BM (1 : 2); (c) ternary blend films of PTB7 : pBTTT : PC_{61}BM with 25 wt% of pBTTT replacing PTB7. All the films were prepared onto glass/ITO/PEDOT : PSS substrates. (d) R_{rms} of the various films as a function of pBTTT content (wt%).

References

[1] I. Etxebarria, J. Ajuria, and R. Pacios, "Polymer: fullerene solar cells: materials, processing issues, and cell layouts to reach power conversion efficiency over 10%, a review," *Journal of Photonics for Energy*, vol. 5, no. 1, Article ID 057214, 2015.

[2] J.-D. Chen, C. Cui, Y.-Q. Li et al., "Single-junction polymer solar cells exceeding 10% power conversion effi ciency," *Advanced Materials*, vol. 27, no. 6, pp. 1035–1041, 2015.

[3] A. R. B. M. Yusoff, D. Kim, H. P. Kim, F. K. Shneider, W. J. Da Silva, and J. Jang, "A high efficiency solution processed polymer inverted triple-junction solar cell exhibiting a power conversion efficiency of 11.83%," *Energy and Environmental Science*, vol. 8, no. 1, pp. 303–316, 2015.

[4] Y. Yang, Z. Zhang, H. Bin et al., "Side-chain isomerization on an n-type organic semiconductor ITIC acceptor makes 11.77% high efficiency polymer solar cells," *Journal of the American Chemical Society*, vol. 138, no. 45, pp. 15011–15018, 2016.

[5] H. Bin, L. Gao, Z. Zhang et al., "11.4% efficiency non-fullerene polymer solar cells with trialkylsilyl substituted 2D-conjugated polymer as donor," *Nature Communications*, vol. 7, Article ID 13651, 2016.

[6] K. Yao, Y.-X. Xu, F. Li, X. Wang, and L. Zhou, "A simple and universal method to increase light absorption in ternary blend polymer solar cells based on ladder-type polymers," *Advanced Optical Materials*, vol. 3, no. 3, pp. 321–327, 2015.

[7] S. Honda, T. Nogami, H. Ohkita, H. Benten, and S. Ito, "Improvement of the light-harvesting efficiency in polymer/fullerene bulk heterojunction solar cells by interfacial dye modification," *ACS Applied Materials and Interfaces*, vol. 1, no. 4, pp. 804–810, 2009.

[8] Z. Sun, K. Xiao, J. K. Keum et al., "PS-b-P3HT copolymers as P3HT/PCBM interfacial compatibilizers for high efficiency photovoltaics," *Advanced Materials*, vol. 23, no. 46, pp. 5529–5535, 2011.

[9] S. Miyanishi, K. Tajima, and K. Hashimoto, "Morphological stabilization of polymer photovoltaic cells by using cross-linkable poly(3-(5-hexenyl)thiophene)," *Macromolecules*, vol. 42, no. 5, pp. 1610–1618, 2009.

[10] L. Derue, O. Dautel, A. Tournebize et al., "Thermal stabilisation of polymer-fullerene bulk heterojunction morphology for efficient photovoltaic solar cells," *Advanced Materials*, vol. 26, no. 33, pp. 5831–5838, 2014.

[11] B. H. Hamadani, D. J. Gundlach, I. McCulloch, and M. Heeney, "Undoped polythiophene field-effect transistors with mobility of 1 cm^2 V^{-1} s^{-1}," *Applied Physics Letters*, vol. 91, no. 24, Article ID 243512, 2007.

[12] I. Mcculloch, M. Heeney, M. L. Chabinyc et al., "Semiconducting thienothiophene copolymers: design, synthesis, morphology, and performance in thin-film organic transistors," *Advanced Materials*, vol. 21, no. 10-11, pp. 1091–1109, 2009.

[13] I. McCulloch, M. Heeney, C. Bailey et al., "Liquid-crystalline semiconducting polymers with high charge-carrier mobility," *Nature Materials*, vol. 5, no. 4, pp. 328–333, 2006.

[14] B. Ebenhoch, S. A. Thomson, K. Genevičius, G. Juška, and I. D. Samuel, "Charge carrier mobility of the organic photovoltaic materials PTB7 and PC71BM and its influence on device performance," *Organic Electronics*, vol. 22, pp. 62–68, 2015.

[15] N. Zhou, H. Lin, S. J. Lou et al., "Morphology-performance relationships in high-efficiency all-polymer solar cells," *Advanced Energy Materials*, vol. 4, no. 3, Article ID 1300785, 2014.

[16] R. L. Uy, S. C. Price, and W. You, "Structure-property optimizations in donor polymers via electronics, substituents, and side chains toward high efficiency solar cells," *Macromolecular Rapid Communications*, vol. 33, no. 14, pp. 1162–1177, 2012.

[17] J. E. Parmer, A. C. Mayer, B. E. Hardin et al., "Organic bulk heterojunction solar cells using poly(2,5-bis(3- tetradecyllthiophen-2-yl)thieno[3,2,- b] thiophene)," *Applied Physics Letters*, vol. 92, no. 11, Article ID 113309, 2008.

[18] N. C. Cates, R. Gysel, Z. Beiley et al., "Tuning the properties of polymer bulk heterojunction solar cells by adjusting fullerene size to control intercalation," *Nano Letters*, vol. 9, no. 12, pp. 4153–4157, 2009.

[19] D. W. Gehrig, I. A. Howard, S. Sweetnam, T. M. Burke, M. D. McGehee, and F. Laquai, "The impact of donor-acceptor phase separation on the charge carrier dynamics in pBTTT:PCBM photovoltaic blends," *Macromolecular Rapid Communications*, vol. 36, no. 11, pp. 1054–1060, 2015.

[20] Z. He, C. Zhong, S. Su, M. Xu, H. Wu, and Y. Cao, "Enhanced power-conversion efficiency in polymer solar cells using an inverted device structure," *Nature Photonics*, vol. 6, no. 9, pp. 591–595, 2012.

[21] J. C. Aguirre, S. A. Hawks, A. S. Ferreira et al., "Sequential processing for organic photovoltaics: design rules for morphology control by tailored semi-orthogonal solvent blends," *Advanced Energy Materials*, vol. 5, no. 11, Article ID 1402020, 2015.

[22] W. Chen, T. Xu, F. He et al., "Hierarchical nanomorphologies promote exciton dissociation in polymer/fullerene bulk heterojunction solar cells," *Nano Letters*, vol. 11, no. 9, pp. 3707–3713, 2011.

[23] E. A. A. Arbab, B. Taleatu, and G. T. Mola, "Environmental stability of PTB7:PCBM bulk heterojunction solar cell," *Journal of Modern Optics*, vol. 61, no. 21, pp. 1749–1753, 2014.

[24] Y. Yang Michael, W. Chen, L. Dou et al., "High-performance multiple-donor bulk heterojunction solar cells," *Nature Photonics*, vol. 9, no. 3, pp. 190–198, 2015.

[25] L. Lu, T. Xu, W. Chen, E. S. Landry, and L. Yu, "Ternary blend polymer solar cells with enhanced power conversion efficiency," *Nature Photonics*, vol. 8, no. 9, pp. 716–722, 2014.

[26] Y. Xiao, H. Wang, S. Zhou et al., "Efficient ternary bulk heterojunction solar cells with PCDTBT as hole-cascade material," *Nano Energy*, vol. 19, pp. 476–485, 2016.

[27] M. Zhang, F. Zhang, J. Wang, Q. An, and Q. Sun, "Efficient ternary polymer solar cells with a parallel-linkage structure," *Journal of Materials Chemistry C*, vol. 3, no. 45, pp. 11930–11936, 2015.

[28] S. Liu, P. You, J. Li et al., "Enhanced efficiency of polymer solar cells by adding a high-mobility conjugated polymer," *Energy and Environmental Science*, vol. 8, no. 5, pp. 1463–1470, 2015.

[29] S. Zhang, L. Zuo, J. Chen et al., "Improved photon-to-electron response of ternary blend organic solar cells with a low band gap polymer sensitizer and interfacial modification," *Journal of Materials Chemistry A*, vol. 4, no. 5, pp. 1702–1707, 2016.

[30] Y. Ohori, S. Fujii, H. Kataura, and Y. Nishioka, "Improvement of bulk heterojunction organic solar cells based on PTB7:PC61BM with small amounts of P3HT," *Japanese Journal of Applied Physics*, vol. 54, no. 4S, pp. 1–8, 2015.

[31] Y. He, G. Zhao, B. Peng, and Y. Li, "High-yield synthesis and electrochemical and photovoltaic properties of indene-C_{70} bisadduct," *Advanced Functional Materials*, vol. 20, no. 19, pp. 3383–3389, 2010.

[32] R. A. Street, D. Davies, P. P. Khlyabich, B. Burkhart, and B. C. Thompson, "Origin of the tunable open-circuit voltage in ternary blend bulk heterojunction organic solar cells," *Journal of the American Chemical Society*, vol. 135, no. 3, pp. 986–989, 2013.

[33] M. Scarongella, J. De Jonghe-Risse, E. Buchaca-Domingo et al., "A close look at charge generation in polymer: fullerene blends with microstructure control," *Journal of the American Chemical Society*, vol. 137, no. 8, pp. 2908–2918, 2015.

[34] N. C. Miller, E. Cho, M. J. N. Junk et al., "Use of X-ray diffraction, molecular simulations, and spectroscopy to determine the molecular packing in a polymer-fullerene bimolecular crystal," *Advanced Materials*, vol. 24, no. 45, pp. 6071–6079, 2012.